A Probabilistic Framework to Detect Suitable Grasping Regions on Objects

Diego R. Faria [*] **Ricardo Martins** [*] **Jorge Lobo** [*] **Jorge Dias** [*] , [**]

[*] *Institute of Systems and Robotics, University of Coimbra (ISR-UC)*
University of Coimbra, Polo II, 3030-290 Coimbra, Portugal
emails: {diego,rmartins,jlobo,jorge}@isr.uc.pt
[**] *Khalifa University, UAE (e-mail: jorge.dias@kustar.ac.ae).*

Abstract: This work relies on a probabilistic framework to search for suitable grasping regions on objects. In this approach, the object model is acquired based on occupancy grid representation that deals with the sensor uncertainty allowing later the decomposition of the object global shape into components. Through mixture distribution-based representation we achieve the object segmentation where the outputs are the point cloud clustering. Each object component is matched to a geometrical primitive. The advantage of representing object components into geometrical primitives is due to the simplification and approximation of the shape that facilitates the search for suitable object region for grasping given a context. Human demonstrations of predefined grasp are recorded and then overlaid on the object surface given by the probabilistic volumetric map to find the contact points of stable grasps. By observing the human choice during the object grasping, we perform the learning phase. Bayesian theory is used to identify a potential object region for grasping in a specific context when the artificial system faces a new object that is taken as a familiar object due to the primitives approximation into known components.

Keywords: Human demonstration, object representation, probabilistic framework, grasping.

1. INTRODUCTION

The ability of handling different objects dexterously is one of the most well succeeded human skills. Artificial perception systems are used in robotics to enable these human actions. Some grasping strategies for robotic systems base on analysing the object geometric properties to fit suitable grasps, others on learning from human demonstrations using specific objects. In this work, we use the object as an object-centric probabilistic volumetric model as in Faria et al. (2010), which is useful here to represent the contact location and forces associated to the grid cell location on the object surface representing successful grasps during the human demonstrations. It will facilitate future matching for an artificial system observing objects and searching for cues on how to grasp an object in a specific context.

Humans usually identify object parts in order to choose a suitable region to grasp. The Recognition By Components theory (RBC) Biederman (1987) reveals that humans are able to identify objects by segmenting them into geometric primitives (geons). Based on that, we use information of daily objects such as global shape and its segmented components to acquire the probability distribution of a graspable part given by human demonstration. The segmentation of the object into components and their approximation using superquadrics decreases the huge amount of potential grasps for that specific object part. This knowledge can be extended for "unknown" objects to estimate the object location and the candidate grasp given the information previously acquired from similar objects. Since an unknown or new object is segmented and approximate to a known geometrical primitive, the system can consider this object similar to other already observed. Fig. 1 shows the flowchart of our proposed system.
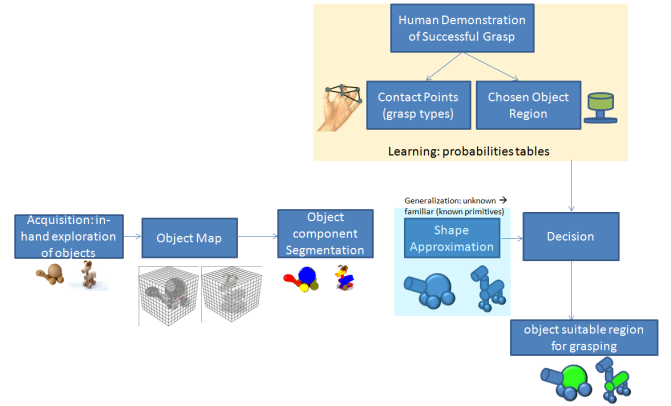

Fig. 1. Flowchart of our proposed framework.

2. RELATED WORK

Researches on human motion and grasping have been carried out for automatic generation of grasping strategy such as Asada and Asari (1988), Kang and Ikeuchi (1995), Kawasaki et al. (2009). Usually many approaches try to find successful grasp given a 3D object model. Some of them associate the object model in specific geometrical primitives, Miller et al. (2003) or fit to superquadrics model, Goldfeder et al. (2007). Thus, it is possible to limit the number of candidate grasps for each primitive. In Hubner and Kragic (2008) for instance, potential grasps are searched through cues provided by the primitives that were associated to a specific object.

Richtsfeld and Vincze (2008) compute grasp points based on the center of mass of the object's top surfaces. The object models are acquired based on range images. Tests with a real robotic

hand were not accomplished, but simulations were carried out to find a proper pose of the end-effector for those contact points. Saxena et al. (2007) proposed a system that infers where to grasp an object using visual information. They apply machine learning techniques to train a grasping point model on labelled synthetic object images. Bohg and Kragic. (2010) shows the analysis of grasping as combination of a descriptor based on visual shape context with a non-linear classification algorithm that leads to a detection of stable grasping points for a variety of objects.

The approach developed by Li and Pollard (2005) depend on the availability of a 3D object model to find a suitable grasp as a shape matching problem between the hand and the object. They use a database of human grasp examples and the object shape features are used to match against the hand postures.

In this work we estimate the regions of the object that are going to be grasped. In our work, a probabilistic framework is used for the representation of 3D objects, which is then segmented in components using Gaussian mixture models as the segmentation demonstrated in Jr. et al. (2010) applied in mobile robotics. Later we approximate each segment in a superquadric model as proposed by El-Khoury and Sahbani (2010). In our representation, we associate data on object graspable parts such as contact points and tactile force obtained from demonstrations of successful stable grasps.

3. OBJECT SHAPE REPRESENTATION

In order to estimate the object region as graspable given a specific context, the combination of human demonstrations of stable grasps and object intrinsic information play an important role for the decision. Since we have the 3D representation of the object in a volumetric map (more details can be seen in previous work Faria et al. (2010)), we can overlay the relevant data through human demonstrations of contact points of stable grasps on the object surface represented in the grid cells of the object map. It also allows the identification of the grasp type by analysing the contact points location and the shape formed by these points.

In this work we are restricting the application for domestic daily objects to test our approach. These objects are used by humans in everyday tasks and can be extended for artificial systems to deal with them by taking decision on which is the proper region to grasp.

3.1 3D Object Global Shape Representation

Since we are extending our previous work Faria et al. (2010) regarding object representation to combine with human demonstration, a fast review is given in this subsection regarding probabilistic representation of the object global shape.

Using magnetic tracker sensors (Polhemus Liberty) in each fingertip of the right hand, the shape of the object can be achieved by performing a contour following procedure on the object surface. These sensors have 6DoF {*x, y, z, yaw, pitch, roll*}. The strategy of this previous work Faria et al. (2010) was to use hand to extract the object geometrical information. Adopting the occupancy grid methodology, the probabilistic volumetric map is computed.

The motivations behind the implementation of this probabilistic map is the intuitive way of static object representation and

the way of dealing with the uncertainty of the sensors. During the finger displacement on the object surface, it is possible to identify in which cell that measurement is inserted (given by the sensors positions). Due to the size of each cell relatively to the standard deviation of the sensors measurements (magnetic tracking system), inside each cell is defined a 3D isotropic Gaussian distribution, $P(Z_{grasp}|O_c)$, centred at the cell central point with standard deviation of 3mm and mean value equal to coordinates of the cell central point. The occupancy of each individual voxel is assumed to be independent from the other voxels and $P(Z_{grasp}|O_C)$ is the distribution corresponding to the set of measurement Z_{grasp} that influences the cell in the map derived from the in-hand exploration data. The probability distribution on the occupation's probability $P(O_C|Z_{grasp})$ for each voxel is computed through Bayesian techniques to updated the cell in the map. More details can be found in Faria et al. (2010).

Fig. 2 shows an example of object representation achieved by using the probabilistic volumetric map derived from in-hand exploration. The cells of the volumetric map (see the middle image) is darker due to that region was more explored than other regions. Due to the way the object was explored (vertical movements: top-down) we can see some pattern represented by the darker cells (vertical cells). Note that in parallel to the darker lines, from one side of the mug to the another side, we have the same pattern of darker cells, it is easily explained due to the thumb and index finger were always in a parallel position during the exploration moving in similar way.
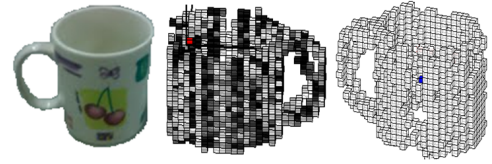

Fig. 2. Object representation using the probabilistic volumetric map: the first image is the object, followed by the probabilistic volumetric map. The last image is the map showing clear cells just those ones occupied (probability higher than the specified threshold 0.7).

3.2 Segmentation of Object Global Shape into Components

Applying the clustering process on the output of the object map to find the object components, we achieve outlier removal and we can keep some object information such as size and position. Using mixture distribution, Gaussian Mixture Models (GMM), we can find the most suitable clustering that will represent an object component.

Gaussian Mixture Models is an efficient methodology for points clustering where each cluster represents a Gaussian function. The density function of the mixture g is defined as follows:

$$g(\mathbf{x}|\Psi) = \sum_{j=1}^{K} w_j c_j(\mathbf{x}, \mu_j, \Sigma_j|\theta_j), \qquad (1)$$

$$\Psi = (w_1...w_K, \theta_1...\theta_K), \qquad (2)$$

and

$$w_j > 0 \;\; \text{and} \;\; \sum_{j=1}^{K} w_j = 1, \qquad (3)$$

where $\mathbf{x} \in \mathbb{R}^3$ containing the contact points, K denotes the number of Gaussian densities and c_j is one of the possible density functions describing a component of the object global shape. Each element of the mixture is weighted by w_j. In this work, Ψ represents the K dimensional vector containing all parameters of the Gaussian mixture and $\theta_j = (\mu_j, \Sigma_j)$ represents a vector containing all the contact points coordinates of the means μ_j and all the entries of the covariance matrix Σ_j. The conditions presented in (3) guarantee that g is indeed a density function.

The estimation of the parameters of each individual density function and the weight variables is accomplished by means of the well known Expectation Maximization (EM) algorithm. In this work, the size of the K is selected using the MDL penalty function Rissanen (1978), where $K_{max} = 3$ (three components are enough to describe different graspable regions on daily objects).

Figure 3 shows an example of daily object (sponge) segmentation using GMM.

After some tests with different daily objects, empirically we know that three segments is enough to represent their shapes. In this work, the K_{max} parameter in the GMM process is set to 3 which can generates since 1 to 3 components depending on the data distribution.
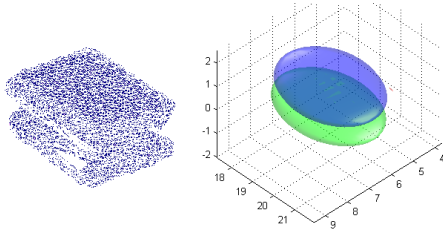

Fig. 3. Object Segmentation using the GMM process. Left image: sponge point cloud; Right: Gaussian density functions.

Fig. 4 shows examples of object segmentation by GMM clustering. The clustering is based on the distribution of the points. The number of points of the object model may influence the segmentation. The same object acquired by the same sensor modality has similar segmentation. The coloured region in each object represents the points belonging to the same cluster. in this example to test the efficiency ogf the segmentation process we have used point cloud from different sensor modalities such as: laser scanner, in-hand exploration (magnetic tracker) and Kinect device.

3.3 Shape Approximation using Superquadrics

The human studies show that segmenting the object shape and associating them to geometrical primitives (geons), we are allowed to identify easily the object components and estimating candidate regions to grasp (for instance, object handle), reducing the possible number of grasp configurations.

For extraction of primitives, in this work we are adopting the known technique namely superquadrics. The advantage of this technique is the higher variety of shape options and also due to the facility of computing the parameters that enclose important cues such as scale and orientation. Superquadrics has been used for 3D object modelling Barr (1981) and for segmentation of point cloud Chevalier et al. (2003), in robotics (novelty
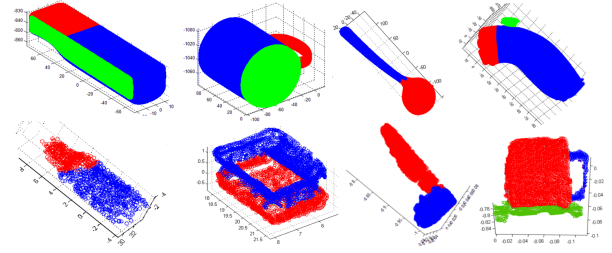

Fig. 4. Daily objects (wii-mote, mug, sponge, bottle, ladle and Nintendo nunchuck) segmentation using GMM. These objects were acquired by different sensor modalities to test the segmentation. Top row: laser scanner; bottom row: in-hand exploration (bottle and sponge); Kinect device (ladle and mug).

detection) Jr. et al. (2010) and successfully in other works for grasping purposes.

After the segmentation process, the points of each Gaussian density function will represent a shape primitive. For that, to estimate the parameters of the superquadric model, the gradient least-square minimization based on Levenberg-Marquardt method Chevalier et al. (2003) is used. More details can be found in Jaklič et al. (2000).

Figures 5 and 6 show examples of superquadrics models achieved using daily objects such as sponge and wii-mote.
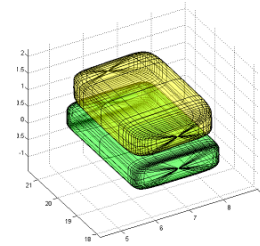

Fig. 5. Object (sponge) shape approximation using superquadrics model. The superquadrics was generated for each component of the object: $prim1$ and $prim2$ = rounded boxes.
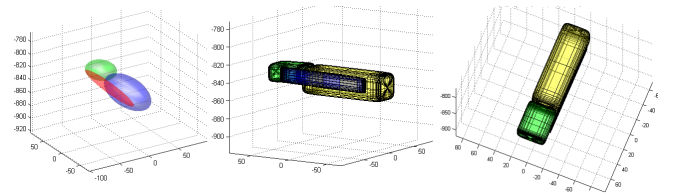

Fig. 6. Object (wii-mote) shape approximation using superquadrics. The superquadrics was generated for each component of the object: $prim1$=box; $prim2$=box; $prim3$=plane

The main contribution of this work is not focused on the object modelling, but it is an important step used to reach the final goal of estimating the suitable region as graspable using also the knowledge acquired from human demonstration.

4. LEARNING OBJECT GRASPABLE REGION FROM HUMAN DEMONSTRATION

Through human demonstrations and object properties information, we can identify types of grasping, contact points locations

of stable grasps as well as the human choice for object graspable region.

In our experimental setup, the data acquisition system records human hand and fingers 6D pose using a magnetic tracking system (Polhemus Liberty), tactile (Tekscan Grip) forces distributed on the inside of the hand. Thus, with the volumetric information of the object we can overlay the contact points given by human demonstrations on the object surface. The forces distribution for each contact point is also kept in each of the respective cell of the object map where the contact point is. This can be used in the future to reproduce stables grasps in a robotic platform. Since we have the volumetric map with the contact points overlaid on the surface of the object, we know the chosen region of the object for grasping.

4.1 Candidate Contact Points on the Object Surface

We keep the contact points location through the 3D positions of the fingers (acquired by the magnetic tracker sensors) when a subject touch the object (i.e. the tactile sensors are active). The contact points location are overlaid on the object surface (cells location in the object map) easily since we are working in the same frame of reference. Our framework also allows multimodal perception, for that, it is needed a calibration process to work in the same frame of reference, e.g. the calibration shown in Faria et al. (2009).

Fig.7 shows examples of contact points overlaid on the object surface. The figure presents some objects grabbed by a human subject with a successful stable grasp during a manipulation task.

contact points during a stable grasp
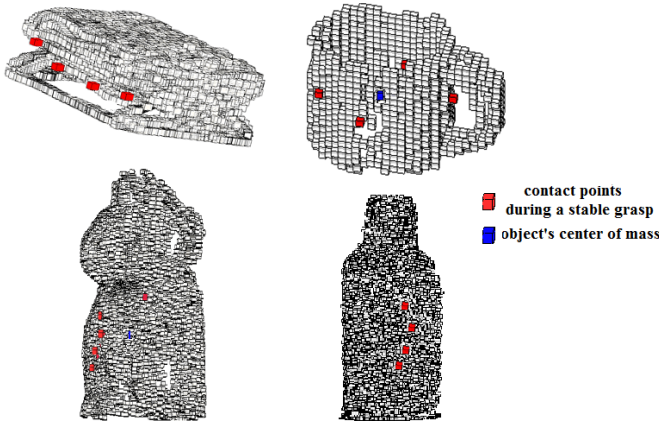object's center of mass

Fig. 7. Examples of contact points of stable grasps from human demonstration on the object surface. The objects are: sponge, mug, wooden cat, bottle.

Other relevant information we have extracted from human demonstrations is the grasp type associated to the disposition of the contact points on the object surface. Given the 3D coordinates of the contact points, we compute the Euclidean distances between the fingertips, i.e. distance between thumb and index, index and middle, and so on. The distances measure of each contact point to the object centroid are also computed, then an average between the contact points distances to the centroid is computed. Adopting the squared mean distance we can define some classes of possible grasp type by analysing a threshold to distinguish each class, e.g. top grasp, side grasp, grasp by handle, etc. The mentioned threshold to associate to a grasp type is found after many observations of the same

grasp type (average). The steps to extract a grasp type given the contact points on the object surface are:

$$D_f = \frac{1}{N} \sum_{i=1}^{N} d_i^2 \qquad (4)$$

where $d = \sqrt{(p_x - q_x)^2 + (p_y - q_y)^2 + (p_z - q_z)^2}$ (Euclidean distance between two fingers).

The same step of (4) is computed for D_c, the distance between a contact point and the object centroid.

Given a new observation of stable grasp, after computed the contact points distances, we can associate it to a pre-defined grasp by:

$$grasp = \begin{cases} 1, & (T_{f\_\min} < D_f < T_{f\_\max}) \ and \\ & (T_{c\_\min} < D_c < T_{c\_\max}) \\ 0, & otherwise \end{cases} \qquad (5)$$

where $grasp \in \{top\text{-}grasp, side\text{-}grasp, grasp\text{-}by\text{-}handle\}$; T_f and T_c are thresholds found by using the standard deviation computed from all contact points representing a grasp type.

In this work we are assuming just three possible candidate grasps for the daily objects to extract relevant information from human demonstration as well as to evaluate the mentioned approach. Given the contact points acquired from the human demonstration, we are associating them into the following classes: top-grasp, side-grasp and grasp-by-handle without paying attention in a detailed grasp taxonomy, e.g. if the grasps are power or precision grip or even in the hand shape to verify if is a cylindrical grasp or any other type. This detailed information is not needed in this work because our main focus is on the decision when the system faces an object to find the most suitable region for grasping. Here we show the possibility of taking advantage of the human demonstration to assist in this approach.

After some trials of human demonstration on how to grasp an object given the objects models and the contexts, we could build a probability table to distinguish what kind of grasping is more probable to happen in each specific situation and also the object region that was chosen for the grasping. Usually the grasp type can be strongly associated to the region of the object, e.g. side grasp happens in the body (middle part) of the object, grasp-by-handle in the designed part of the object to grasp (the handle of a mug, umbrella or bucket), and top grasp happens in the top region of an object. An example is shown in Fig. 8 where we can see the possible grasps during three different tasks: pick-up and place, pick-up and pour and pick-up and lift. In these trials a mug was used. The object orientation for all trials was the handle of the object turned to the right side to the subjects view. The orientation of the object can influence the choice of grasping.

4.2 Learning Object Graspable Region in Task-oriented Grasps

Given a set of observations to represent a specific task $\mathscr{T}$, with $\mathscr{T} \in \{$pick-up and place; pick-up and lift; pick-up and pour/tilt$\}$, we have the probability of each type of grasp represented as $P(G|\mathscr{T})$. The probability distribution for each type of grasp $g \in G$ is computed as follows:
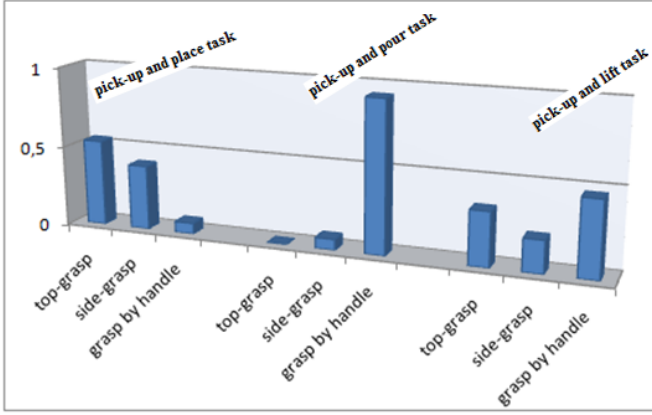
Fig. 8. Chosen Grasps in different contexts: Grasps types were detected as well as the object region that was chosen for the initial grasp. Probability tables were built observing the occurrences of grasp types and the object region that was chosen given the context.

$$P(g_i) = \frac{g_i}{G}. \qquad (6)$$

where g_i is the number of occurrences of a specific grasp type and G is the total number of possible grasps.

To identify the object graspable region we verify the locations of the contact points on the object surface and then we know that position is associate to a specific superquadric model that represents a component of an object. Given a set of observations to represent a task $\mathcal{T}$, we have the probability of each object component (geometrical primitive represented by a superquadric model) $C \in \{prim_1, prim_2, prim_3\}$ being the graspable region $P(C|\mathcal{T})$. It is computed in a similar way as shown in (6) where each component of the object has a probability associated to be the graspable region given the context by computing the occurrences based on humans' choices for the object region defined as graspable.

Fig.9 shows some learned tables of the chosen object graspable part after the human demonstration. The three objects shown (mug, bottle and wii-mote) have three components; the chosen primitive is the object component with higher probability after multiples observation.

Based on the learning phase, some analysis can be carried out, for instance, observing the human choice given a combination of superquadrics models. Instead of keeping just the probability table achieved during the learning associated to an specific component of object such as mug, bottle, etc., we can store the priorities given the combination of primitives based on those probabilities. When a mug is used during the human demonstration, we can use the combination of primitives such as cylinder-cylinder-bend cylinder, storing the human choice for this combination. Other example is the bottle, it can be represented as a combination of three cylinders, each one with an associated probability. This way, in the future, since we cannot recognize the object, for example, given a unknown object, after the mixture distribution-based process and the superqadrics models representation, we can achieve a combination of known primitives, and through this information we can search for the exact stored combination achieved during the demonstration/learning or at least for a similar one, that is, some combination that encloses at least one similar primitive to be possible to use the
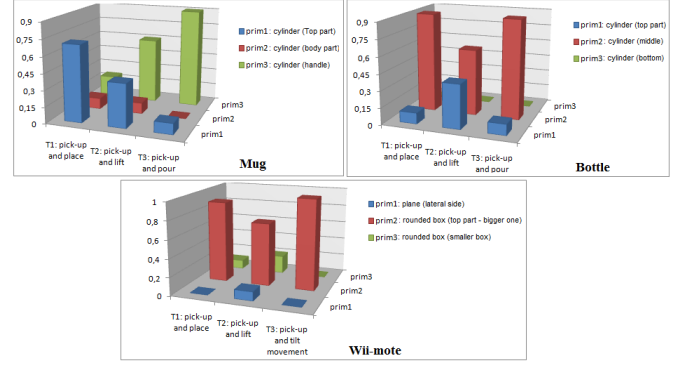

Fig. 9. Learned table of object graspable part. Three different tasks performed many times by 5 different individuals. By analysing the probability distribution of the chosen primitives to perform the grasp we can estimate the object graspable part given the task context. For the mug the three primitives represents a cylinder, the same for the bottle. The wii-mote is composed of 2 boxes primitives and a primitive representing a plane.

probability of the graspable component to take a decision on which component of the object to grasp.

5. OBJECT GRASPABLE REGION IDENTIFICATION

The object graspable region can be identified applying the Bayes theorem. Given a task context $\mathcal{T}$, to identify the object graspable region C, first is needed to detect the object geometrical primitives c. The probability distributions are obtained from the occurrence statistics acquired with the datasets of the given task.

Given a context $\mathcal{T}$, we can estimate the object graspable part C as follows:

$$P(C = c_i|\mathcal{T}) = \frac{P(\mathcal{T}|C = c_i)P(C = c_i)}{\sum_j P(\mathcal{T}|C = c_j)P(C = c_j)} \} \qquad (7)$$

where the posterior information $P(C = c_i | \mathcal{T}C)$ is computed for each primitive C of the object in a specific task $\mathcal{T}$; the likelihood $P(\mathcal{T}C|C = c_i)$ is the learned probability for each primitive of the object given a task context as explained in the previous sub-section. The normalisation factor is the sum of the probability of each object primitive being the graspable region.

A basic example of this application is given during the grasping planning, when a robot needs to execute a task. After detecting the object and its geometrical primitives, using the learned information from human demonstrations, the robot can identify the object graspable region for possible suitable grasps.

After learning a set of objects and task context, when the object is observed again in the same context, the system is able to detect the graspable part as shown in figure 10. The graspable component is chosen according to the maximum a posteriori (MAP) estimate.

In case of unknown objects, we have adopted a generalisation process, reusing the prior knowledge for other contexts, for instance, if a unknown object has one primitive in common with a known object, a similar grasp can be attempted. The unknown object falls to a familiar object, i.e. after the object segmentation process (applying the superquadrics model), this
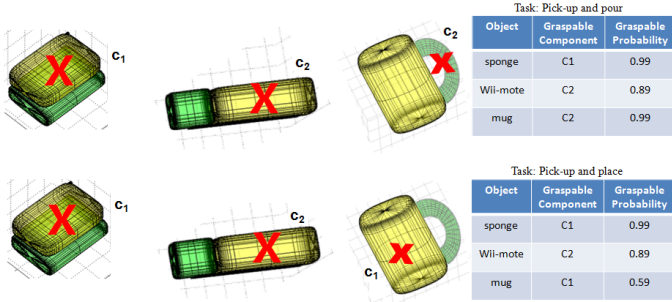
Fig. 10. Identification of object graspable parts for the sponge, *wii-mote* and mug. Each component has a probability of being graspable, the maximum a posteriori estimate indicates the graspable component in each context.

object will have known geometrical primitives. Given a task, a Bayesian classification as shown in (7) is computed for each object primitive to infer the most probable object primitive for that task.

The feasibility and the quality of the work is somehow dependently on how a given object is represented after the segmentation and how its components are matched to a specific model. This way, the system can generate the hypotheses of regions on objects being graspable.

6. CONCLUSION AND FUTURE WORK

The outputs of this work can be used as a strategy in robotic applications for grasping purposes. A volumetric map of the object was used to overlay the partially observed volume of the object with data about human hand-object contact points and tactile forces which helps to identify the chosen region of the object for grasping. Preliminary results suggest the suitability to find a graspable region given an object model and the context since we acquire relevant observed information on how to grasp an object. The segmentation of the object into components will facilitate future matching for an artificial system observing objects and searching for data on how to perform successful grasps inside a specific context. The segmentation step shows to be promising, but it is strongly dependent of the point cloud distribution. The Bayesian theory shows to be a good option to estimate the object region for grasping. In future work we intend to extend this framework to deal also with contact points and their generalization for unknown objects and test the object grasping with a real robot hand using a quality measure.

ACKNOWLEDGEMENTS

REFERENCES

Asada, H. and Asari, Y. (1988). The direct teaching of tool manipulation skills via the impedance identification of human motion. In *IEEE ICRA*.

Barr, A.H. (1981). Superquadrics and angle preserving transformations. In *IEEE Computer Graphics and Applications, 1(1):1123*.

Biederman, I. (1987). Recognition-by-components: A theory of human image understanding. *Psychological Review*, 94, 115–147.

Bohg, J. and Kragic., D. (2010). Learning grasping points with shape context. *Robotics and Autonomous Systems*, 58(4), 362–377.

Chevalier, L., Jaillet, F., and Baskurt, A. (2003). Segmentation and superquadric modeling of 3d objects. *WSCG*, 11, 232–239.

El-Khoury, S. and Sahbani, A. (2010). A new strategy combining empirical and analytical approaches for grasping unknown 3d objects. *robotics and Autonomous Systems*, 58(5), 497–507.

Faria, D.R., Martins, R., Lobo, J., and Dias, J. (2010). Probabilistic representation of 3d object shape by in-hand exploration. In *IEEE/RSJ Int. Conf. Intelligent Robots and Systems*.

Faria, D.R., Aliakbarpour, H., and Dias, J. (2009). Grasping movements recognition in 3d space using a bayesian approach. In *The 14th Int. Conf. on Advanced Robotics*.

Goldfeder, C., Allen, P.K., Lackner, C., and Pelossof, R. (2007). Grasp planning via decomposition trees. In *IEEE Int. Conf. on Robotics and Automation*.

Hubner, K. and Kragic, D. (2008). Selection of robot pre-grasps using box-based shape approximation. In *IEEE Int. Conf. on Intelligent Robots and Systems*.

Jaklič, A., Leonardis, A., and Solina, F. (2000). *Segmentation and Recovery of Superquadrics*, volume 20. Kluwer.

Jr., P.D., Nunez, P., Rocha, R., Campos, M., and Dias., J. (2010). Novelty detection and 3d shape retrieval using superquadrics and multi-scale sampling for autonomous mobile robots. In *IEEE ICRA'10. ISBN 978-1-4244-5040-4/10*.

Kang, S.B. and Ikeuchi, K. (1995). Toward automatic robot instruction from perception-temporal segmentation of tasks from human hand motion. *IEEE Trans. on Robotics and Automation*, 11, 670–681.

Kawasaki, H., Furukawa, T., Ueki, S., and Mouri, T. (2009). Robot teaching based on motion analysis and hand manipulability for multi-fingered robot. *Journal of Advanced Mechanical Design, Systems, and Manufacturing*, 3, 1–12.

Li, Y. and Pollard, N. (2005). A shape matching algorithm for synthesizing humanlike enveloping grasps. In *5th IEEE-RAS Int.Conf. on Humanoid Robots*, 442–449.

Miller, A.T., Knoop, S., Christensen, H.I., and Allen, P.K. (2003). Automatic grasp planning using shape primitives. In *IEEE Int. Conf. on Robotics and Automation*.

Richtsfeld, M. and Vincze, M. (2008). Grasping of unknown objects from a table top. In *ECCV Workshop on Vision in Action: Efficient strategies for cognitive agents in complex environments*.

Rissanen, G. (1978). Modeling the shortest data description. *Automatica*, 14, 465–471.

Saxena, A., Driemeyer, J., Kearns, J., and Ng, A.Y. (2007). Robotic grasping of novel objects. *Neural Information Processing Systems*, 19, 12091216.